

## Supporting Information

### Interfacial Interactions between Protective, Surface-Engineered Shells and Encapsulated Bacteria with Different Cell Surface Composition

Hao Wei, Xiao-Yu Yang, Wei Geng, Henny C. van der Mei\*, Henk J. Busscher\*

**Bacterial surface composition:** XPS modelling of the bacterial cell surface composition was based on a previously published method, that assumes that the bacterial cell surface is composed of proteins, polysaccharides and lipoteichoic acids.<sup>1</sup> Based on the ratios in which N, O and P occur with respect to C in these three model compounds, measured elemental surface ratios N/C, O/C and P/C were related with those of model compounds, according to:

$$N/C = 0.270 \times C_{Pr} + 0.200 \times C_{Pg} \quad (1)$$

$$O/C = 0.320 \times C_{Pr} + 1.200 \times C_{Ta} + 0.833 \times C_{Ps} \quad (2)$$

$$P/C = 0.170 \times C_{Ta} \quad (3)$$

$$1 = C_{Pr} + C_{Pg} + C_{Ta} + C_{Ps} + C_{Ch} \quad (4)$$

$C_{Pr}$ ,  $C_{Pg}$ ,  $C_{Ta}$ ,  $C_{Ps}$  and  $C_{Ch}$  represent the elemental surface concentrations of protein, peptidoglycan, teichoic acid, polysaccharide and hydrocarbon-like compounds, respectively. Hydrocarbon-like compounds here predominantly relate to unavoidable carbon contamination in the XPS, while peptidoglycan was neglected as a surface component as it resides quite deep (relative to the XPS depth of information) into the cell wall.

**Table S1.** Concentrations of key-chemicals in each encapsulation method applied in this work that are in direct contact with the bacterial cell surface. Concentrations were derived based on maintaining maximal viability of the encapsulated strains.

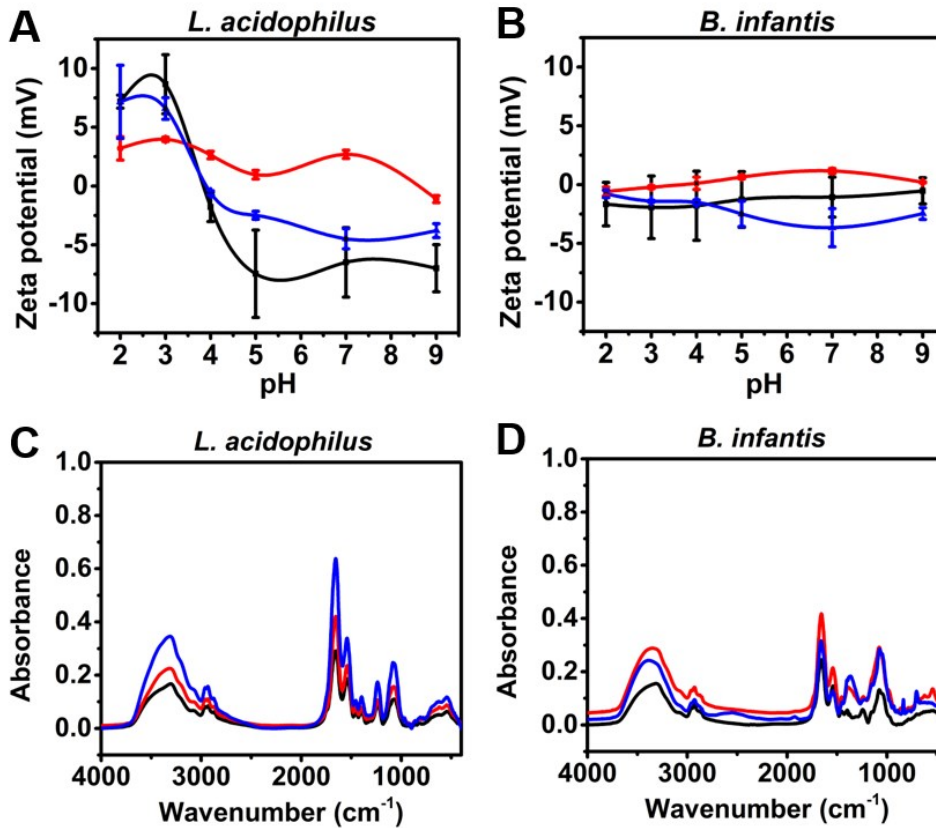
<b><i>L. acidophilus</i> ATCC 4356</b>	
<b>ZIF-8 biomineralization</b>	0.16 M dimethylimidazole and 0.04 M zinc acetate
<b>Alginate gelation</b>	2.5 wt% sodium alginate
<b>Protein assisted SiO<sub>2</sub> nanoparticles packing</b>	2 mg mL <sup>-1</sup> protamine sulfate and 5 mg mL <sup>-1</sup> SiO <sub>2</sub>
<b><i>B. infantis</i> ATCC 15697</b>	
<b>ZIF-8 biomineralization</b>	0.16 M dimethylimidazole and 0.04 M zinc acetate
<b>Alginate gelation</b>	2.5 wt% sodium alginate
<b>Protein assisted SiO<sub>2</sub> nanoparticles packing</b>	1 mg mL <sup>-1</sup> protamine sulfate and 1 mg mL <sup>-1</sup> SiO <sub>2</sub>

**Table S2.** Elemental surface compositions of *L. acidophilus* and *B. infantis* surfaces prior to and after adsorption of protamine sulfate, obtained using XPS.

Cell surface	Elemental surface composition (at%)					
	C	N	O	P	Na	S
<b>Protamine adsorption to <i>L. acidophilus</i> ATCC 4356</b>						
Prior to adsorption	66.2	12.2	19.2	2.5	-	-
Immediately after adsorption	63.8	13.6	21.5	-	0.3	0.8
60 min after adsorption	62.6	10.7	22.5	0.7	1.0	-
<b>Protamine adsorption to <i>B. infantis</i> ATCC 15697</b>						
Prior to adsorption	63.1	1.7	34.6	0.6	-	-
Immediately after adsorption	53.8	8.3	30.5	1.0	2.5	1.6
60 min after adsorption	66.3	3.9	27.7	-	1.4	-

**Table S3.** Ionic character, Molecular Weight (MW) and Minimal Inhibitory Concentrations (MIC) of the antibiotics involved in this study against *L. acidophilus* ATCC 4356 and *B. infantis* ATCC 15697.

	<b>Tobramycin</b>	<b>Amoxicillin</b>	<b>Tetracycline</b>
<b>Ionic character</b>	Positive	Zwitter-ionic	Negative
<b>MW (Da)</b>	468	420	444
<b>MIC (<math>\mu\text{g mL}^{-1}</math>) <i>L. acidophilus</i></b>	64	0.25	8
<b>MIC (<math>\mu\text{g mL}^{-1}</math>) <i>B. infantis</i></b>	64	0.25	2



— Prior to protamine adsorption

— Immediately after protamine adsorption

— 60 min after protamine adsorption

**E**

Samples	Aml/CH	AmlI/CH
<b><i>L. acidophilus</i> ATCC 4356</b>		
Prior to protamine adsorption	4.0	1.7
Immediately after protamine adsorption	5.4	1.9
60 min after protamine adsorption	5.7	1.6
<b><i>B. infantis</i> ATCC 15697</b>		
Prior to protamine adsorption	3.0	1.3
Immediately after protamine adsorption	4.9	1.3
60 min after protamine adsorption	4.2	0.6

**Figure S1.** Zeta potentials and infrared absorption bands of *L. acidophilus* ATCC 4356 and *B. infantis* ATCC 15697 prior to and after protamine sulfate adsorption. **(A)** Bacterial zeta potential of *L. acidophilus* prior to, immediately after and 60 min after protamine adsorption. **(B)** Same as panel **(A)**, now for *B. infantis*. **(C)** FTIR absorption spectrum of *L. acidophilus* prior to, immediately after and 60 min after protamine adsorption. **(D)** Same as panel **(C)**, now for *B. infantis*. **(E)** FTIR amide I ( $1653\text{ cm}^{-1}$ ) and amide II ( $1541\text{ cm}^{-1}$ ), absorption band ratios with respect to the C-H absorption stretching band between  $2815\text{ cm}^{-1}$  and  $3006\text{ cm}^{-1}$  of *L. acidophilus* and *B. infantis* prior to, immediately after and 60 min after adsorption. The FTIR spectra were scaled to similar base-line levels. All error bars indicate standard deviations over triplicate experiments with separately cultured and encapsulated bacteria.

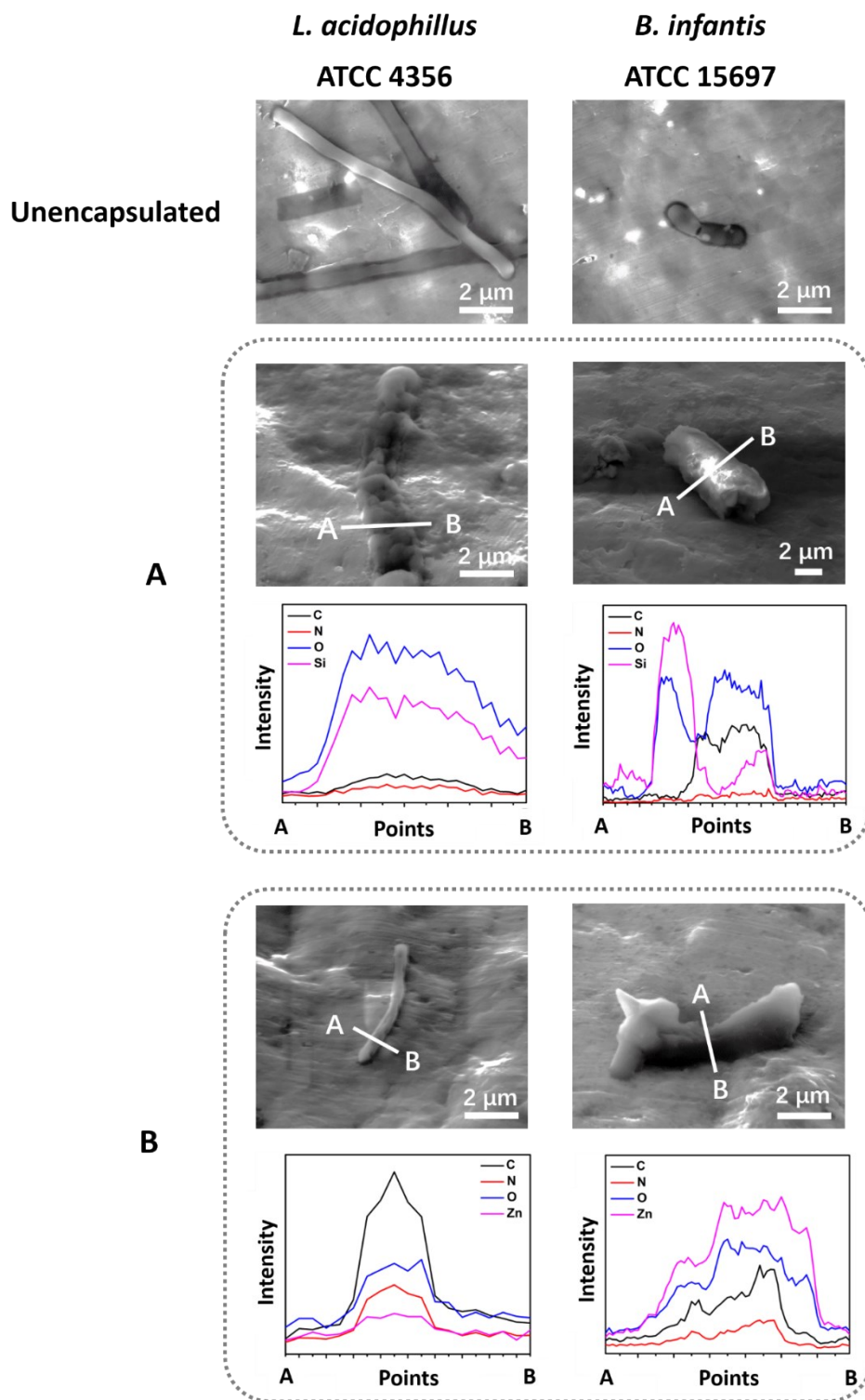


**Figure S2.** SEM micrographs and EDX line scans along the indicated A to B white lines in the micrographs and resulting elemental compositions of unencapsulated and differently encapsulated *L. acidophilus* ATCC 4356 and *B. infantis* ATCC 15697. **(A)** Protamine-assisted yolk-shell packing of SiO<sub>2</sub> nanoparticles. **(B)** ZIF-8 biomineralization.

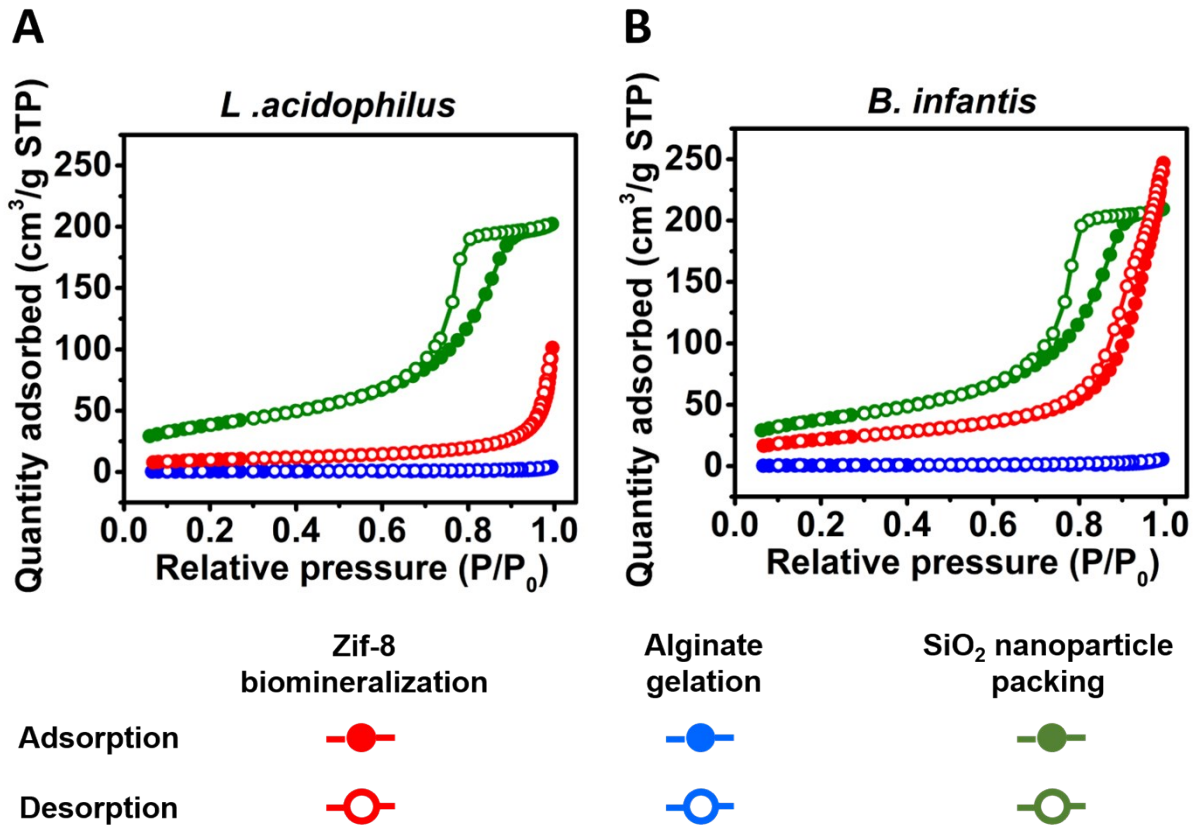


**Figure S3.** Nitrogen adsorption/desorption isotherms of differently encapsulated (A) *L. acidophilus* ATCC 4356 and (B) *B. infantis* ATCC 15697.

## References

- 1 H. C. Van der Mei, J. De Vries and H. J. Busscher, *Surf. Sci. Rep.*, 2000, **39**, 1-24.